

Surface Roughness and Tool Wear during Single-Point Diamond Turning of Rapidly Solidified Aluminium Alloys

J.K. Belgraver¹, W.H. Kool², J.M. Oomen³

¹ Present address: KBM Master Alloys B.V., Delfzijl, The Netherlands

² Department of Materials Science and Engineering, Delft University of Technology, Rotterdamseweg 137, 2628 AL Delft, The Netherlands (corresponding author: w.h.kool@tnw.tudelft.nl)

³ Philips Research Laboratories, Prof. Holstlaan 4 (WD01), 5656 AA Eindhoven, The Netherlands

Keywords: rapid solidification, meltspinning, high-precision machining, surface roughness

Abstract

Many materials show superior properties after solidification with cooling rates of 10^5 - 10^6 °C/s. Such high cooling rates provide a structural refinement and an improvement of properties such as ductility, formability, strength, corrosion resistance and machinability. Possible applications for rapidly solidified Al-based alloys are pistons and products requiring high strength or high wear resistance. The refined microstructure might also be beneficial for ultraprecision machining. In this study several rapidly solidified Al alloys were machined using single-point diamond turning. Surface roughness and tool wear were compared with those of conventionally processed alloys. The use of rapidly solidified Al alloys generally resulted in lower tool wear and/or lower surface roughness.

1. Introduction

Ultraprecision machining enables the production of optical, electrical or mechanical components within shape tolerance of 50 nm and surface roughness (R_{\max}) of 10 nm or less [1]. Ultraprecision machining is performed by single-point diamond turning (SPDT). Ultimate surface roughness is primarily determined by the quality of lathe and tooling in combination with temperature control of the environment but, these aspects being optimal, the influence of material properties such as the presence of coarse intermetallic compounds or grain size will become noticeable. For instance, for technical aluminium alloys, the best values of R_a and R_{\max} which might be obtained, are 20 nm and 100 nm respectively. A further improvement of the surface roughness is often obtained by diamond turning of a deposited electroless nickel layer, for which a surface roughness of 0.5-9 nm (RMS-value) is reported [2]. The technique of rapid solidification processing (RSP) with cooling rates up to 10^6 °C/s, is a viable technique [3-4] and RSP Al alloys are now commercially available [5]. Since rapid solidification processing strongly refines the microstructure, it might be expected that ultimate surface roughness will improve by machining alloys, which have been fabricated with this technology. In order to verify this idea, several Al alloys, both conventional or rapidly solidified, were machined as well as one highly alloyed RSP piston-type alloy.

2. Experimental

The Al alloys investigated were AA 5083 (C and R), AA 6082 (C and R), AA 2024 (C and R), AA 7075 (C and R) and AlSi23 R, containing 23 w/o Si, 5 w/o Fe and 2 w/o Ni. C and R denote conventional and rapidly solidified material, respectively. The rapidly solidified materials were prepared by melting ingot material and subsequent meltspinning. Rotational speed of the water cooled wheel was $1500 \text{ rev. min}^{-1}$. Thickness of the obtained ribbon was 80 - 100 μm and the width was about 3 mm. After cutting and compacting, the preform was put into the container of a backward laboratory extrusion press. Container diameter of the press was 62 mm and with an extrusion ratio of 17:1, a cylindrical rod of 15 mm diameter was extruded and fully consolidated. Extrusion temperatures were 355 °C (5083 R, 6082 R and 2024 R) and 420 °C (7075 R and AlSi23 R). The 2024, 6082 and 7075 alloys were heat treated for maximum strength (T6) and the AlSi23 alloy was stress relieved. The 5083 alloy was used in the as extruded condition. Conventional materials were obtained by melting ingot material and casting in cylindrical steel moulds with diameter of 55 mm. Then, the alloys were extruded in the same extrusion press as used for the R materials at an extrusion temperature of 420 °C. Heat treatment of the conventional alloys was taken identical to that of the corresponding R alloys. For the ultraprecision machining experiments, specimens with a diameter of 14.5 mm and height of 30 mm were machined from the rod.

The machining experiments were performed on a numerically controlled lathe having two hydrostatic slides in a T-base arrangement, see Figure 1. One slide contained the specimen. An air-bearing spindle was used for the specimen rotation around its central axis (z direction) which corresponded to the extrusion direction of the sample. The movement of the slide was also in this direction with a positioning accuracy of 0.05 μm . The specimen was machined in its front plane. The other slide moved parallel to the front plane of the specimen (x direction) and contained the diamond tool. The positioning accuracy of the tool in this direction was 0.5 μm . The entire setup is similar to that described earlier [1,6]. The lathe was located in an air-conditioned room at constant temperature of 20 °C in order to suppress the effects of thermal expansion. The slide

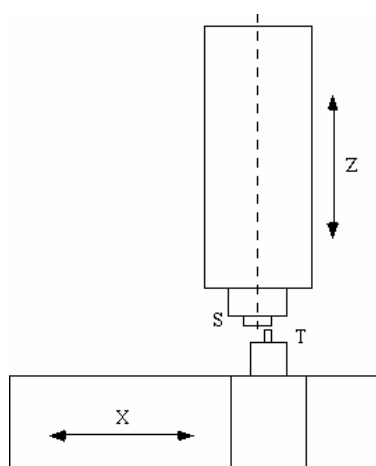


Figure 1: Schematic of the lathe. T: diamond tool; S: specimen; X and Z indicate movements in x and z direction.

containing the tool carried a dynamometer to measure the cutting forces in three orthogonal directions. The operating range of this dynamometer was from 1 mN to 100 N. Vibrational frequencies above 60 s^{-1} were filtered out. Further details are given elsewhere [1]. Tooling used for this study consisted of type Ia diamonds, involving commonly used natural diamonds, which contain relatively large amounts of nitrogen [1]. Orientation and geometry were as follows: rake plane orientation: (001); clearance surface: normal to [100]; rake angle: 0°; clearance angle: 5°; wedge angle: 85° and nose tip radius: 1 mm.

In the experiments a fully sharp diamond tool was used for each experiment. Machining of the specimen took place from edge to centre in a repeated movement and, while going from centre to edge, the tool was withdrawn. Transverse force F_f , main cutting force F_c and thrust force F_p (x, y and z direction, respectively) were measured at regular intervals with the tool at

a position near the edge of the specimen. Cutting speed at this location was 2.8 m/s. The machining parameters were as follows: rotational speed specimen: 3650 rev./min; feed rate: 5 $\mu\text{m}/\text{rev.}$; depth of cut: 5 μm ; cutting speed: 2.8 m/s (edge) - 0.2 m/s (centre); total cutting length: 5 10^4 m; lubrication: spray of Isolube. In all cases single-point diamond turning resulted in mirror-like surfaces.

Surface roughness was measured after machining a short distance with a fully sharp diamond tool as well as after machining a total cutting length of 5 10^4 m. A Taylor-Hobson Talystep surface profiler was used. The profile was measured near the edge of the specimen in radial direction over a sampling length of 1.25 mm. Any low frequency component was filtered out which resulted in a height contour varying around a zero baseline. Over the sampling length, the difference R_{max} between height maximum and height minimum as well as R_a were determined. R_a was defined as the averaged absolute value of h , where h is height with respect to baseline.

Tool wear was measured after machining a total distance of 5 10^4 m by pressing the tool into a rotating annealed Cu disk at a rate of 1 $\mu\text{m}/\text{rev.}$ The resulting contour was determined with the Talystep surface profiler and compared with the contour determined for the fully sharp tool [1].

3. Results

Hardness data are summarized in Figure 2. The trend over the various alloys follows the expected behaviour. In most cases hardness for RSP materials is slightly higher, due to their smaller grain size. Highest hardness is for the AlSi23 R alloy due to the presence of numerous Si particles and AlFeSi or AlFeNi phases. Optical microscopy, electron probe micro-analysis and transmission electron microscopy reveal the microstructural refinement as a result of the rapid solidification. Grain size for the conventionally processed alloys is in the range of 50-200 μm whereas it is 4 μm or less for the RSP alloys. In the conventionally processed alloys several large (15-20 μm) particles are present, in contrast with the RSP alloys, which only contain small (≤ 2 μm) precipitates or intermetallic phases in much higher quantities. The number of these large particles in the conventionally processed alloys ranges from 3-9 10^{-3} μm^{-2} depending on the alloy type. In the first stage of machining a continuous chip is formed for all alloys except AlSi23 R. At larger cutting distance, short chips are obtained since the chips fracture by the larger deformations imposed, as a consequence of the tool blunting. For AlSi23 R pulverised 'chips' are formed because of the presence of numerous small Si, AlFeSi and AlFeNi particles.

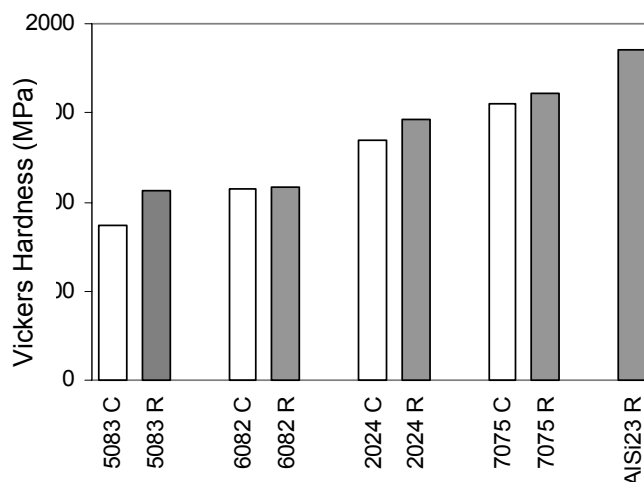


Figure 2: Hardness of the various alloys.

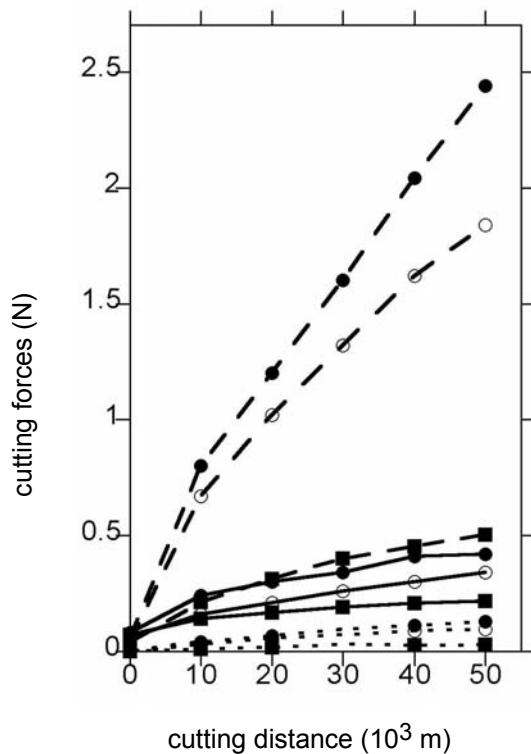


Figure 3: Thrust force F_p (---), main cutting force F_c (—) and transverse force F_f (.....) versus cutting distance for 6082 C (o), 6082 R (●) and AlSi23 R (■).

All the three cutting forces F_c , F_p and F_f increase against cutting distance due to increasing tool wear. Figure 3 shows typical paths for some alloys. In Figure 4 cutting forces are given after a cutting distance of $5 \cdot 10^4$ m. It appears that these forces may differ by a factor of 10 from one alloy to another. Cutting forces are high for the 2024 R and low for the AlSi23 R alloy. The sequence of the other alloys, going from high to low cutting forces, is 6082 R, 6082 C, 2024 C, 7075 (C and R similar), 5083 C and 5083 R. However, maximum force variation in this sequence is only a factor of two.

Tool wear gradually increases for all alloys against cutting distance. The tool wear found after a total cutting distance of $5 \cdot 10^4$ m is shown in Figure 5. It is seen that tool wear is highest for the 2024 R alloy and lowest for

the AlSi23 R alloy, which are also the alloys with the highest and lowest cutting forces. Figure 6a shows surface roughness R_a after machining a short distance with a fully sharp diamond tool and after machining a total cutting distance of $5 \cdot 10^4$ m. R_a is always 10

nm or less. Often, R_a is somewhat smaller when using a sharp cutting tool. In most cases R_a values are lower for the RSP alloys. Figure 6b presents similar data of the surface roughness R_{max} . R_{max} values for the RSP alloys are always lower than those of the corresponding conventional alloys. Optical microscopy of the machined surfaces,

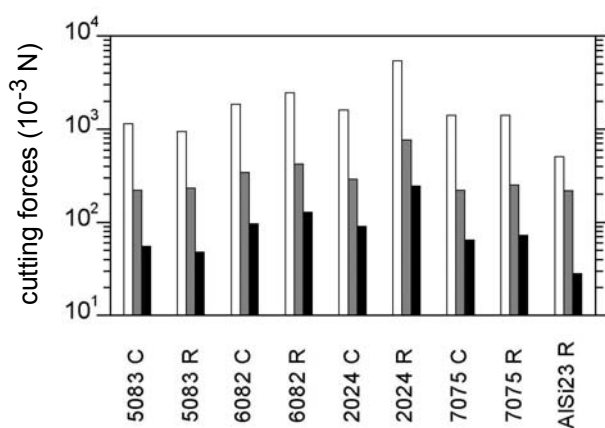


Figure 4: Thrust force F_p (□), main cutting force F_c (■) and transverse force F_f (■) after a cutting distance of $5 \cdot 10^4$ m.

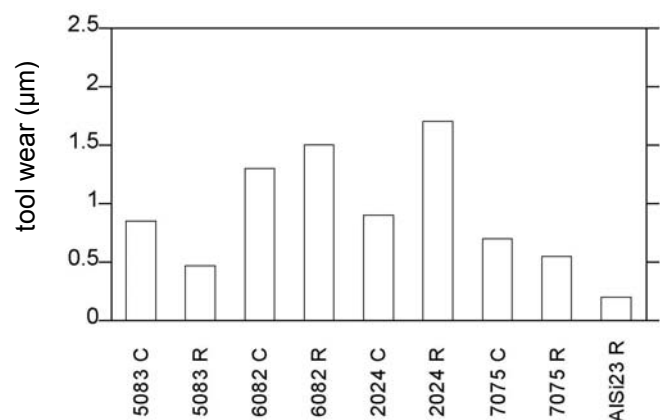


Figure 5: Tool wear for the various alloys after a cutting distance of $5 \cdot 10^4$ m.

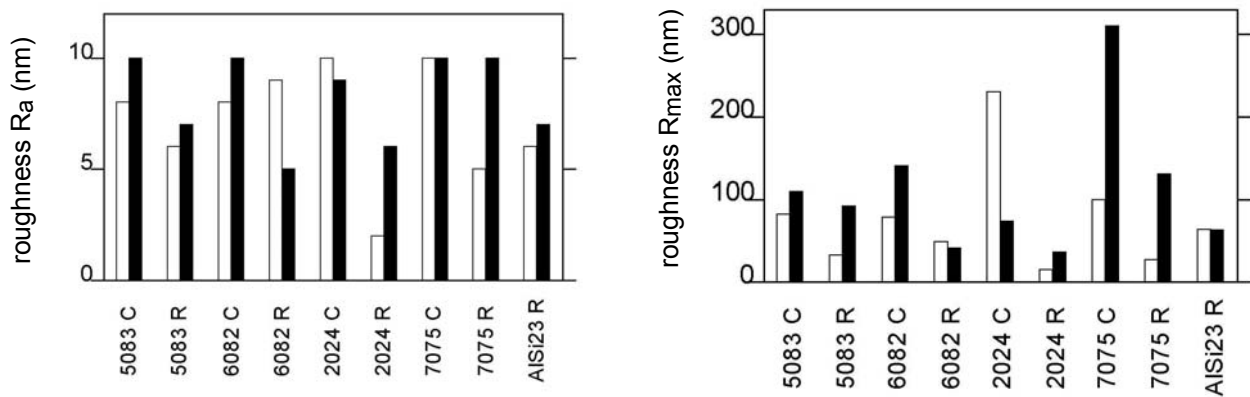


Figure 6: Surface roughness R_a (left) and R_{max} (right) for the various alloys; (□): machined with fully sharp tool; (■): after a cutting distance of $5 \cdot 10^4$ m.

under interference contrast, reveals typical differences between the conventional and the rapidly solidified alloys. An example is given in Figure 7. In general the conventionally processed alloys show many coarse ($\sim 15 \mu\text{m}$) constituents, either still present in the surface or broken out. Machining grooves are sometimes visible (5083 C, 7075 C) or invisible (6082 C, 2024 C). In contrast the RSP alloys show only a few constituents of $\sim 2 \mu\text{m}$ or less except for the AlSi23 R alloy which contains numerous small ($\sim 2 \mu\text{m}$) Si particles. For the RSP alloys machining grooves are clearly visible.

4. Discussion

In Figure 8 tool wear is plotted against main cutting force F_c after a cutting distance of $5 \cdot 10^4$ m for the various alloys studied. It appears that for the conventional alloys a linear trend is followed as indicated by the dotted line. The intersection with the abscissa corresponds with the (averaged) value of F_c , found at zero cutting distance. The tool wear for the rapidly solidified alloys is generally found below this line. The lower tool wear is attributed to the absence of coarse intermetallic phases or constituents. Alloy AlSi23 R gives rise to a very low tool wear. Due to numerous small brittle phases in this alloy, chips leave in pulverised form as a powder, which lowers friction at the rake face and therefore minimizes tool temperature despite the high hardness of the alloy.

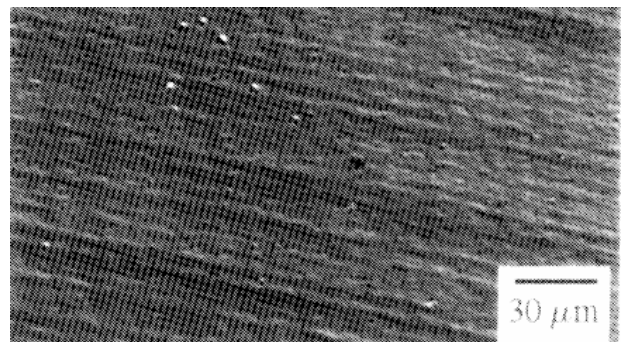
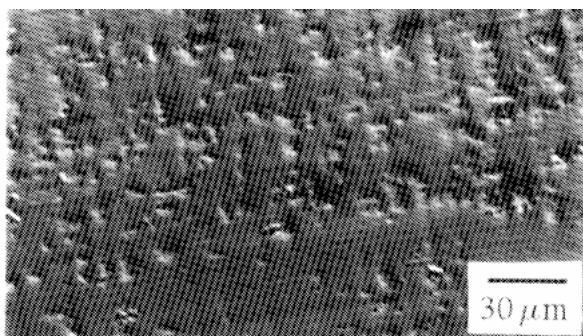


Figure 7: Optical micrographs (interference contrast) of the machined surface after a cutting distance of $5 \cdot 10^4$ m. Left: 2024 C; right: 2024 R.

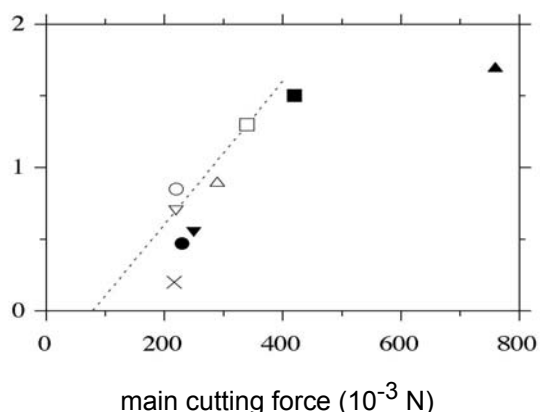


Figure 8: Tool wear vs F_c ; cutting distance: $5 \cdot 10^4$ m. 5083 (C,o; R,●), 6082 (C,□; R,■), 2024 (C,△; R,▲), 7075 (C,▽; R,▼) and AlSi23 R (X). Dotted line: see text.

Figure 9 shows tool wear after a cutting distance of $5 \cdot 10^4$ m plotted against surface roughness R_a and R_{max} . Rapidly solidified alloys are identified in the regions with the lowest tool wear and with the lowest surface roughness. They provide the best combination of low tool wear and low roughness. The same holds after machining with a sharp tool. This confirms earlier results [3] that the refined microstructure of rapidly solidified alloys is beneficial and improves the machining quality.

5. Conclusion

Due to rapid solidification the microstructure of Al alloys is refined resulting in a smaller grain size and in an absence of larger inclusions or intermetallic phases, which are common in conventionally processed alloys.

Single-point diamond turning of rapidly solidified Al alloys results in lower tool wear and/or lower surface roughness.

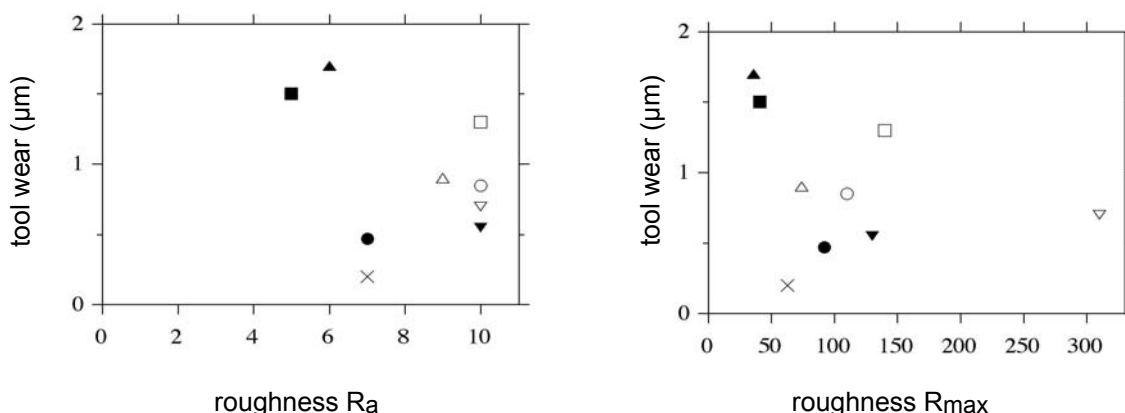


Figure 9: Tool wear vs roughness; cutting distance: $5 \cdot 10^4$ m. for R_a (above) and R_{max} (below). 5083 (C,o; R,●), 6082 (C,□; R,■), 2024 (C,△; R,▲), 7075 (C,▽; R,▼) and AlSi23 R (X).

References

- [1] J.M. Oomen and J. Eisses, Precision Engineering 4, 14 (1992) 206-218
- [2] C.K. Syn, J.S. Taylor and R.R. Donaldson in Proc. SPIE Techn. Symp. on Ultraprecision Machining and Automated Fabrication of Optics, San Diego, CA, USA (1986) vol. 676 (1987) 128-140
- [3] W.H. Kool, H. Kleinjan, F.A.C.M. Habraken and J.H. Dautzenberg in Proc. 27th Int. Symp. on Automotive Technology and Automation (ISATA) -New and Alternative Materials for the Transportation Industries- Automotive Automation Ltd, Croydon, UK (1994) 253-260
- [4] W.H. Kool, H. Kleinjan, F.A.C.M. Habraken and J.H. Dautzenberg, Materialen 5 (1995) 15-20
- [5] RSP Products, Rotterdam, The Netherlands
- [6] T.G. Gijsbers, Philips Techn. Rev. 39 (1980) 229-244